EPI International Journal of Engineering
Volume 7, Number 2, August 2024, pp. 58-67
DOI: 10.25042/epi-ije.082024.03

*p*ISSN 2615-5109
*e*ISSN 2621-0541

Vibration Analysis of Simply Supported Rectangular Plates Constrained by Rotational Edge Springs

Yoshihiro Narita[a,*]

[a]Hokkaido University (Professor Emeritus), N-13, W-8, Sapporo, Japan. Email: ynarita1951@gmail.com

Abstract

Comprehensive and accurate numerical results are presented for natural frequencies of thin isotropic, simply supported rectangular plates additionally constrained by rotational elastic springs on the edges. For complete coverage of combination, the number of all the combinations in boundary conditions of simply supported, rotationally constrained and clamped is calculated by Polya counting theory, and all sets of frequency parameters are tabulated for the lowest five modes. The Ritz method, along with displacements assumed in special polynomial form with boundary index, is used to include the strain energy stored in the rotational springs. Convergence and comparison studies are made to demonstrate accuracy of tabulated results, and the frequency parameters are listed for the fifteen sets of boundary conditions and various spring stiffness of the square plates. Some results are also presented for rectangular plates.

Keywords: Free vibration, natural frequency, simply supported plate, rectangular plate, rotational spring

1. Introduction

Vibration of flat plates has been an important research topic in mechanical, aeronautical and other structure-oriented fields in engineering. A large number of publications has appeared since a monograph was compiled by Leissa [1] in 1969, and some good textbooks were released, for example a book written by Gorman [2] on plate vibration. Among various plate applications, the most typical planform is a rectangle, and Leissa [3] published a paper on frequency parameters to cover all combinations of free, simply supported and clamped edges. These results are updated by the present author in improved accuracy [4].

For rectangular plates elastically constrained along edges, a reasonable number of papers were published because of the importance that plate structural elements are usually attached elastically to the main structure. Up to the year of 2000, Laura and his co-workers published some papers [5-8] to obtain lower frequencies, and other authors [9,10] dealt with plates with springs. A series of notable works were written by Gorman [11-15] on vibration of rectangular plates with elastic edge supports by using a famous method of the superposition method.

In the 2000's, Li [16] and Li [17] presented solutions for predicting frequencies of rectangular plates with generally restrained edges. Eftekhari and Jafari [18] derived a solution for variable thickness plates with elastic edges. Recently, Wan [19] presented an original analysis on the topic, and Zhang and others [20] presented in 2021 some results on plates with free and opposite two adjacent elastic edges. Leng and others [21] studied in 2022 vibration of plates with one corner free and its edges rotationally-restrained. Thus, up to now, the vibration of rectangular plates with elastic edge springs has drawn attentions from researchers, but the purpose of all the previous papers seems to propose analytical methods, and the frequency data presented are still limited to some specific cases.

The present author therefore undertakes to compile comprehensive and organized sets of frequency parameters for the problem, and published already one paper [22] on the free plates elastically supported by translational springs. In this paper, an analysis is extended to simply supported rectangular plates with rotational spring on the edges. These two papers fully encompass elastically supported rectangular plates in a way to cover

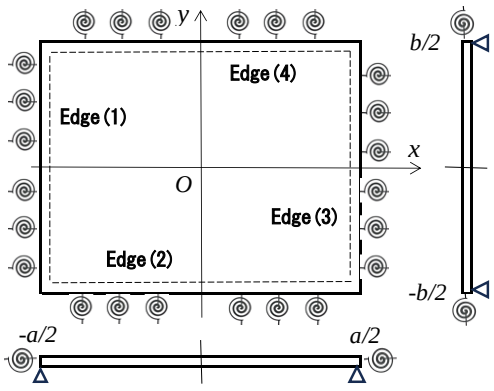

Figure 1. Simply supported rectangular plate with uniform rotational springs on the edges and the coordinate system

*Corresponding author.
N-13, W-8, Kitaku
Sapporo, Japan, 060-8628

from a totally free to a simply supported plate [22] and from there to a totally clamped plate (present paper).

2. Methodology

2.1. Combination of boundary conditions

Figure 1 illustrates an isotropic rectangular plate simply supported along four edges and elastically constrained by additional uniform rotational spring at the edges, and this edge condition is denoted by RS (Rotational Spring) in the paper. The dimension of the plate is given by $a \times b \times h$ (thickness) and the origin of the coordinate system is located in the center. Starting from the left hand edge ($x = -a/2$), four edges are labelled as Edge(1), Edge(2), Edge(3) and Edge(4) in counter-clock-wise, and each spring can have different value of rotational spring stiffness.

When one considers combination of the classical boundary conditions (F, S, C) in an isotropic square plate ($a/b=1$), there are twenty-one combinations to give distinct sets of the identical natural frequencies and this number can be theoretically determined by use of Polya counting theory [23,24]. In this theory, the number of combinations is determined by a cyclic polynomial

$$Z_G(z) = \frac{1}{8}\left(z^4 + 2z^3 + 3z^2 + 2z\right) \tag{1}$$

where Z_G is the number of distinct combinations to show independent sets of different natural frequencies, *G* denotes "permutation", and *z* is the number of different boundary conditions considered at each edge. For example, when one considers three boundary conditions (Free (F), Simple support (S), Clamp (C)), the number "three" is inserted in Eq.(1) as $Z_G(3) = 21$.

In this paper, three combinations of S, RS and C are considered that end up with $Z_G(3) = 21$, but the combinations only by S and C (i.e., z=2) were already covered [4] and remaining fifteen cases

$$Z_G(3) - Z_G(2) = 21 - 6 = 15 \tag{2}$$

are treated in numerical examples, as shown as Ex.1-15 in Fig. 2.

For an isotropic rectangular plate ($a/b \neq 1$), a cyclic polynomial becomes

$$Z_G(z) = \frac{1}{4}\left(z^4 + 2z^3 + z^2\right) \tag{3}$$

and the number of combinations increases up to

$$Z_G(3) = 36 \tag{4}$$

for the combination of S, RS and C [23,24].

2.2. Ritz method considering rotational edge springs

A semi-analytical solution is employed here as in Refs.[4,22,23] from the method of Ritz under the classical thin plate theory. The relation between stress and strain in the plate is

$$\begin{Bmatrix} \sigma_x \\ \sigma_y \\ \tau_{xy} \end{Bmatrix} = \begin{bmatrix} Q_{11} & Q_{12} & 0 \\ Q_{12} & Q_{22} & 0 \\ 0 & 0 & Q_{66} \end{bmatrix} \begin{Bmatrix} \varepsilon_x \\ \varepsilon_y \\ \gamma_{xy} \end{Bmatrix} \tag{5}$$

with the matrix elements given by

$$Q_{11} = Q_{22} = \frac{E}{1-\nu^2},\ Q_{12} = \nu Q_{11},\ Q_{66} = G = \frac{E}{2(1+\nu)} \tag{6}$$

where *E* is Young's modulus, *G* is a shear modulus and ν is a Poisson's ratio. When Eq.(5) is integrated through the thickness after multiplying a thickness coordinate *z*, one gets moment resultants

$$\begin{Bmatrix} M_x \\ M_y \\ M_{xy} \end{Bmatrix} = \begin{bmatrix} D_{11} & D_{12} & 0 \\ D_{12} & D_{22} & 0 \\ 0 & 0 & D_{66} \end{bmatrix} \begin{Bmatrix} \kappa_x \\ \kappa_y \\ \kappa_{xy} \end{Bmatrix} \tag{7}$$

in terms of curvature $\{\kappa_x, \kappa_y, \kappa_{xy}\}$.

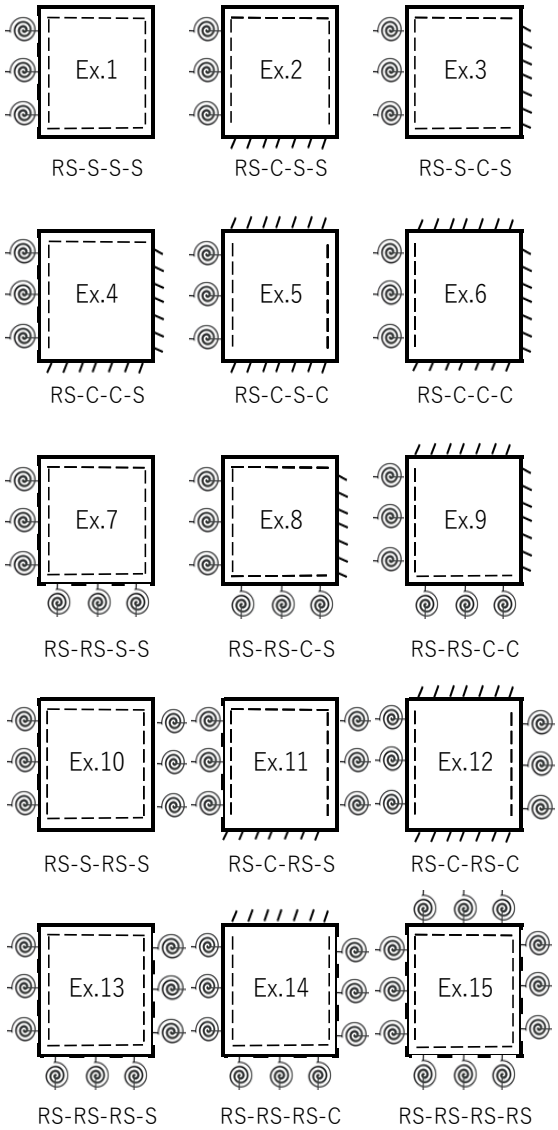

Figure 2. Fifteen numerical examples dealt in the paper

(RS: Rotational Spring, S: Simple support, C: Clamp)

If one considers the small amplitude (linear) free vibration of plate, the deflection w may be written by

$$w(x,y,t) = W(x,y)\sin\omega t \tag{8}$$

where W is the amplitude and ω is a radian frequency of the plate. Then, the maximum strain energy due to the bending is expressed by

$$U_{\max} = \frac{1}{2}\iint_A \{\kappa\}^T \begin{bmatrix} D_{11} & D_{12} & 0 \\ D_{12} & D_{22} & 0 \\ 0 & 0 & D_{66} \end{bmatrix} \{\kappa\}\, dA \tag{9}$$

where the D_{ij} are the bending stiffnesses and $\{\kappa\}$ is a curvature vector

$$\{\kappa\} = \left\{ -\frac{\partial^2 W}{\partial x^2} \quad -\frac{\partial^2 W}{\partial y^2} \quad -2\frac{\partial^2 W}{\partial x \partial y} \right\}^T \tag{10}$$

The maximum kinetic energy is also given by

$$T_{\max} = \frac{1}{2}\rho h \omega^2 \iint_A W^2 dA \tag{11}$$

where ρ [kg/m^3] is the mass per unit volume.

For the sake of simplicity, non-dimensional quantities are introduced as

$$\begin{aligned} &\xi = \frac{2x}{a}, \eta = \frac{2y}{b} \text{ (non-dimensional coordinates),} \\ &\alpha = a/b \text{ (aspect ratio)}, \quad d_{ij} = D_{ij}/D \\ &D = \frac{Eh^3}{12(1-\nu^2)} \text{ (reference stiffness)} \\ &\Omega = \omega a^2 \sqrt{\frac{\rho h}{D}} \text{ (frequency parameter)} \end{aligned} \tag{12}$$

Next, we consider the energy stored in the elastic restraints (rotational elastic springs). The energy equation is written as

$$\begin{aligned} U_r = \frac{1}{2}\times & \left\{ \int_{-b/2}^{b/2} k_{r1} \left[\frac{\partial W(-a/2, y)}{\partial x} \right]^2 dy + \int_{-a/2}^{a/2} k_{r2} \left[\frac{\partial W(x, -b/2)}{\partial y} \right]^2 dx \right. \\ & \left. + \int_{-b/2}^{b/2} k_{r3} \left[\frac{\partial W(a/2, y)}{\partial x} \right]^2 dy + \int_{-a/2}^{a/2} k_{r4} \left[\frac{\partial W(x, b/2)}{\partial y} \right]^2 dx \right\} \end{aligned} \tag{13}$$

where k_{ri} (i=1,2,3,4) are stiffness of rotational springs in unit [Nm/m]=[N] per unit edge length. This energy is added to the plate bending energy (9).

The next step in the Ritz method is to assume the amplitude as

$$W(\xi,\eta) = \sum_{m=0}^{M-1} \sum_{n=0}^{N-1} A_{mn} X_m(\xi) Y_n(\eta) \tag{14}$$

where A_{mn} are unknown coefficients, and $X_m(\xi)$ and $Y_n(\eta)$ are the functions modified so that any kinematical boundary conditions are satisfied at the edges [4,22,23].

After substituting Eq.(14) into these energies, the stationary value is obtained by

$$\begin{aligned} &\frac{\partial}{\partial A_{\bar{m}\bar{n}}} \left\{ T_{\max} - \left(U_{\max} + U_{r,\max} \right) \right\} = 0 \\ &\left(\bar{m} = 0,1,2,..(M-1); \bar{n} = 0,1,2,...(N-1) \right) \end{aligned} \tag{15}$$

Then the eigenvalue equation that contains a frequency parameter Ω is derived as

$$\begin{aligned} &\sum_{m=0}^{M-1} \sum_{n=0}^{N-1} \left[d_{11} I^{(2200)} + \alpha^2 d_{12} (I^{(2002)} + I^{(0220)}) + \alpha^4 d_{22} I^{(0022)} \right. \\ &\left. + 4\alpha^2 d_{66} I^{(1111)} + (\text{Spring term}) - \left(\frac{\Omega^2}{16} \right) I^{(0000)} \right]_{m\bar{m}n\bar{n}} \cdot A_{mn} \\ &= 0 \qquad \left(\bar{m} = 0,1,2,..(M-1); \bar{n} = 0,1,2,...(N-1) \right) \end{aligned} \tag{16}$$

where an integral I is the products

$$I^{(pqrs)}_{m\bar{m}n\bar{n}} = \varphi^{(pq)}_{m\bar{m}} \cdot \varphi^{(rs)}_{n\bar{n}} \tag{17}$$

of the two integrals defined by

$$\phi^{(pq)}_{m\bar{m}} = \int_{-1}^{1} \frac{\partial^{(p)} X_m}{\partial \xi^{(p)}} \frac{\partial^{(q)} X_{\bar{m}}}{\partial \xi^{(q)}} d\xi \tag{18}$$

and (Spring term) is the line integral along an edge.

$$\begin{aligned} (\text{spring} \quad \text{term}) = \frac{1}{2}\times & \left[k^*_{r1} \frac{dX_m(-1)}{d\xi} \int_{-1}^{1} Y_n(\eta) d\eta + k^*_{r2} \frac{dY_n(-1)}{d\eta} \int_{-1}^{1} X_m(\xi) d\xi \right. \\ & \left. + k^*_{r3} \frac{dX_m(1)}{d\xi} \int_{-1}^{1} Y_n(\eta) d\eta + k^*_{r4} \frac{dY_n(1)}{d\eta} \int_{-1}^{1} X_m(\xi) d\xi \right] \end{aligned} \tag{19}$$

with nondimensional rotational constant

$$k^*_{r1} = \frac{k_{r1} a}{D}, k^*_{r2} = \frac{k_{r2} a}{D}, k^*_{r3} = \frac{k_{r3} a}{D}, k^*_{r4} = \frac{k_{r4} a}{D} \tag{20}$$

Equation (16) is a set of linear simultaneous equations in terms of the coefficients A_{mn}, and the eigenvalues Ω may be extracted by using existing computer subroutines.

The present approach uses simple polynomials

$$\begin{aligned} X_m(\xi) &= \xi^m (1+\xi)^{bc1} (1-\xi)^{bc3} \\ Y_n(\eta) &= \eta^n (1+\eta)^{bc2} (1-\eta)^{bc4} \end{aligned} \tag{21}$$

(bc1=bc2=bc3=bc4=1) to represent a simply supported plate as a base plate, and the integrals (18)(19) can be exactly calculated.

2.3. Finite element formulation of rotational spring

A finite element is newly developed to include the effect of rotational springs distributed along the edges, and the finite element code (FEM code) is developed by the author to compare the result with the Ritz solution to establish accuracy of both methods. Formulation of plate bending element and kinetic element are already explained in Refs.[22,25]. Here only formulation of the edge spring element is shown.

The amplitude inside the element including boundary is assumed by

$$W(x,y)=\{P\}\{\alpha\} \tag{22}$$

where $\{P\}$ and $\{\alpha\}$ are (T: transpose)

$$\{P\}=\{1,x,y,x^2,xy,y^2,x^3,x^2y,xy^2,y^3,x^3y,xy^3\} \tag{23}$$

$$\{\alpha\}=\{\alpha_1,\alpha_2,\alpha_3,\alpha_4,\alpha_5,\alpha_6,\alpha_7,\alpha_8,\alpha_9,\alpha_{10},\alpha_{11},\alpha_{12}\}^T \tag{24}$$

The displacement at node i is defined as

$$\{\delta_i\}=\{W_i,(\partial W/\partial x)_i,(\partial W/\partial y)_i\}^T \tag{25}$$

and the displacements of four nodes labelled as *i*,*j*,*k* and *l* in a rectangular element can be expressed as

$$\{\delta_e\}=\{\delta_i \quad \delta_j \quad \delta_k \quad \delta_l\}^T \tag{26}$$

Using [*C*] which is obtained by substituting Eq.(26) into the four sets of node coordinates, *W* is transformed as

$$W(x,y)=\{P\}[C]^{-1}\{\delta_e\} \tag{27}$$

For example, when the rotational spring is distributed uniformly along Edge(2) or Edge(4) at $y=\bar{y}$, equation (27) is substituted into the second or fourth term of Eq.(13) and

$$\frac{1}{2}\int_{-a/2}^{a/2}k_{ri}\left(\frac{\partial W(x,\bar{y})}{\partial y}\right)^2dx=\frac{1}{2}\{\delta_e\}^T\left[K_{ri}\right]\{\delta_e\} \tag{28}$$

(*i*=2,4) is obtained, where [K_{ri}] is the *i*-th finite element of rotational edge spring

$$\left[K_{ri}\right]=k_{ri}\left[C^{-1}\right]^T\left(\int\left\{\frac{\partial P(x,\bar{y})}{\partial y}\right\}^T\left\{\frac{\partial P(x,\bar{y})}{\partial y}\right\}dx\right)\left[C^{-1}\right] \tag{29}$$

with $P(x,\bar{y})$ being a function of *x* at fixed $\bar{y}=-b/2$ or $\bar{y}=b/2$ for Edge(2) and Edge (4), respectively. Spring finite elements along Edge(1) and Edge(3) can be formulated in the same manner.

3. Numerical examples and discussions

3.1. Convergence and comparison of the solution

It is assumed in numerical examples that the material is isotropic with Poisson's ratio ν=0.3. Young's modulus *E* and Poisson's ratio ν are included in the dimensionless frequency parameters Ω in Eq.(12).

Figure 2 illustrates numerical examples Ex.1-Ex.15 with different degree of elastic constraints by rotational springs, and such edge (i.e., simply supported edge with uniform rotational spring attached) is denoted by "RS" (Rotational Spring). In case that the example plates have plural rotational springs on the edges, it is assumed that all the springs have the same degree of constraint.

Table 1 Convergence of (a) Ritz solution and (b)FEM solution for square plates constrained by rotational spring (Ex.1)

	Ω_1	Ω_2	Ω_3	Ω_4	Ω_5
(a) Present Ritz solution					
$k_t^*=100$					
6×6	23.37	51.44	57.75	85.28	101.5
8×8	23.37	51.44	57.74	85.27	100.1
10×10	23.37	51.44	57.74	85.27	100.1
$k_t^*=10000$					
6×6	23.64	51.67	58.65	86.14	101.7
8×8	23.64	51.67	58.64	86.13	100.3
10×10	23.64	51.67	58.64	86.13	100.3
(b) Present FEM solution					
$k_t^*=100$					
10×10	23.24	50.98	57.31	83.61	99.16
15×15	23.31	51.21	57.53	84.47	99.61
20×20	23.33	51.31	57.62	84.81	99.80
$k_t^*=10000$					
10×10	23.51	51.26	58.21	84.63	99.55
15×15	23.58	51.45	58.42	85.32	99.83
20×20	23.62	51.54	58.51	85.65	100.0

Table 2 Comparison of frequency parameters for square plates (Ex.15)

	Ω_1	Ω_2	Ω_3	Ω_4	Ω_5
$k_t^*=1$					
Ritz	21.502	51.191	51.191	80.828	100.58
[17]	21.500	51.187	51.187	80.816	100.58
$k_t^*=10$					
Ritz	28.50	60.22	60.22	90.81	111.19
[17]	28.50	60.22	60.22	90.81	111.19
[16]	28.50	60.22	60.22	90.81	111.2
$k_t^*=100$					
Ritz	34.671	70.781	70.781	104.45	127.03
[17]	34.671	70.780	70.780	104.45	127.02
[16]	34.67	70.78	70.78	104.5	127.0
$k_t^*=1000$					
Ritz	35.843	73.104	73.104	107.79	131.06
[17]	35.842	73.103	73.103	107.79	131.06

$$k_r^*=k_{r1}\left(\frac{a}{D}\right)=k_{r2}\left(\frac{a}{D}\right)=k_{r3}\left(\frac{a}{D}\right)=k_{r4}\left(\frac{a}{D}\right) \tag{30}$$

in the calculation, although they can take any different values as needed.

In the figure, Ex.1-6 are square plates constrained on Edge(1) by one rotational spring, and have different combinations of RS-S-S-S, RS-C-S-S, RS-S-C-S, RS-C-C-S, RS-C-S-C and RS-C-C-C, respectively, on the remaining three edges of Edge(2)-Edge(4). Similarly, Ex.7-12 are plates constrained on two edges constrained by two rotational springs and have different combinations

Table 3 Frequency parameters Ω of square plates
(**Ex.1**, RS-S-S-S, ν=0.3)

kr^*		Ω_1	Ω_2	Ω_3	Ω_4	Ω_5
(0)	Ritz	19.74	49.35	49.35	78.96	98.70
S-S-S-S	FEM	19.71	49.24	49.24	78.54	98.47
1	Ritz	20.18	49.53	50.09	79.43	98.79
	FEM	20.16	49.43	49.99	79.01	98.56
10	Ritz	21.95	50.43	53.74	81.95	99.31
	FEM	21.92	50.32	53.63	81.53	99.07
100	Ritz	23.37	51.44	57.74	85.27	100.1
	FEM	23.33	51.31	57.62	84.81	99.80
10000	Ritz	23.64	51.67	58.64	86.13	100.3
	FEM	23.62	51.54	58.51	85.65	100.0
(infinity)	Ritz	23.65	51.67	58.65	86.13	100.3
C-S-S-S	FEM	23.61	51.53	58.52	85.63	99.99

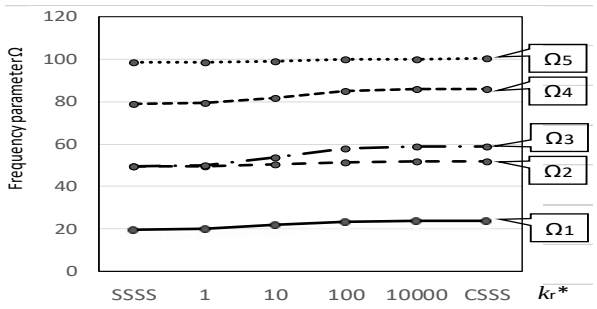

Figure 3 Variation of frequency parameters of square plate with spring stiffness (**Ex.1**).

Table 4 Frequency parameters Ω of square plates
(**Ex.2**, RS-C-S-S, ν=0.3)

kr^*		Ω_1	Ω_2	Ω_3	Ω_4	Ω_5
(0)	Ritz	23.65	51.67	58.65	86.13	100.3
S-C-S-S	FEM	23.61	51.53	58.52	85.63	99.99
1	Ritz	24.02	52.38	58.80	86.57	101.1
	FEM	23.98	52.24	58.67	86.06	100.8
10	Ritz	25.54	55.89	59.57	88.89	105.9
	FEM	25.49	55.75	59.43	88.38	105.6
100	Ritz	26.80	59.75	60.47	92.02	112.8
	FEM	26.75	59.60	60.32	91.46	112.5
10000	Ritz	27.05	60.53	60.78	92.83	114.5
	FEM	27.00	60.38	60.63	92.26	114.2
(infinity)	Ritz	27.05	60.54	60.79	92.84	114.6
C-C-S-S	FEM	27.00	60.37	60.62	92.23	114.2

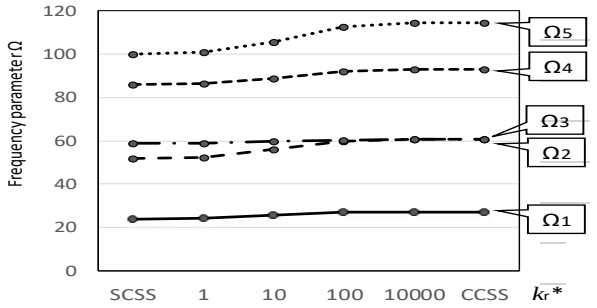

Figure 4 Variation of frequency parameters of square plate with spring stiffness (**Ex.2**).

Table 5 Frequency parameters Ω of square plates
(**Ex.3**, RS-S-C-S, ν=0.3)

kr^*		Ω_1	Ω_2	Ω_3	Ω_4	Ω_5
(0)	Ritz	23.65	51.67	58.65	86.13	100.3
S-S-C-S	FEM	23.61	51.53	58.52	85.63	99.99
1	Ritz	24.21	51.91	59.44	86.67	100.4
	FEM	24.18	51.77	59.31	86.16	100.1
10	Ritz	26.56	53.08	63.48	89.57	101.0
	FEM	26.51	52.93	63.35	89.06	100.7
100	Ritz	28.55	54.42	68.22	93.54	102.0
	FEM	28.50	54.25	68.07	92.98	101.6
10000	Ritz	28.95	54.74	69.32	94.57	102.2
	FEM	28.89	54.57	69.16	94.00	101.9
(infinity)	Ritz	28.95	54.74	69.33	94.59	102.2
C-S-C-S	FEM	28.89	54.55	69.17	93.96	101.9

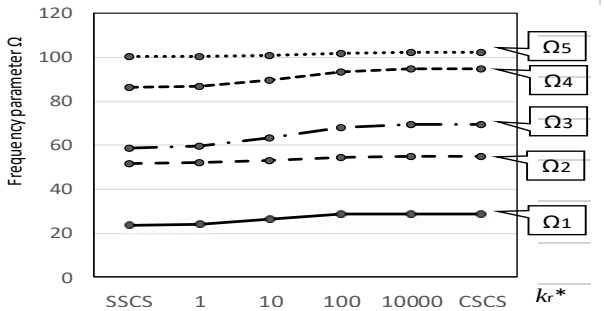

Figure 5 Variation of frequency parameters of square plate with spring stiffness (**Ex.3**).

Table 6 Frequency parameters Ω of square plates
(**Ex.4**, RS-C-C-S, ν =0.3)

kr^*		Ω_1	Ω_2	Ω_3	Ω_4	Ω_5
(0)	Ritz	27.05	60.54	60.79	92.84	114.6
S-C-C-S	FEM	27.00	60.37	60.62	92.23	114.2
1	Ritz	27.55	60.84	61.45	93.33	114.7
	FEM	27.50	60.68	61.28	92.72	114.4
10	Ritz	29.63	61.86	65.35	96.04	115.3
	FEM	29.57	61.69	65.19	95.43	115.0
100	Ritz	31.46	63.04	69.98	99.79	116.1
	FEM	31.39	62.85	69.80	99.13	115.8
10000	Ritz	31.82	63.33	71.06	100.8	116.4
	FEM	31.76	63.13	70.88	100.1	116.0
(infinity)	Ritz	31.83	63.33	71.08	100.8	116.4
C-C-C-S	FEM	31.75	63.11	70.88	100.1	116.0

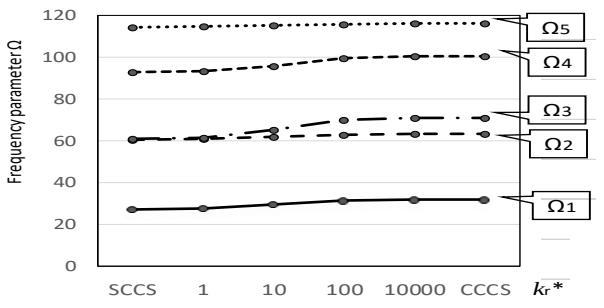

Figure 6 Variation of frequency parameters of square plate with spring stiffness (**Ex.4**).

Table 7 Frequency parameters Ω of square plates

(**Ex.5**, RS-C-S-C, ν =0.3)

kr^*		Ω_1	Ω_2	Ω_3	Ω_4	Ω_5
(0)	Ritz	28.95	54.74	69.33	94.59	102.2
S-C-S-C	FEM	28.89	54.55	69.17	93.96	101.9
1	Ritz	29.26	55.41	69.46	94.98	103.0
	FEM	29.20	55.23	69.30	94.36	102.7
10	Ritz	30.52	58.74	70.12	97.11	107.8
	FEM	30.46	58.56	69.95	96.49	107.4
100	Ritz	31.61	62.47	70.89	100.0	114.5
	FEM	31.54	62.27	70.70	99.35	114.2
10000	Ritz	31.82	63.32	71.07	100.8	116.3
	FEM	31.75	63.12	70.89	100.1	116.0
(infinity)	Ritz	31.83	63.33	71.08	100.8	116.4
C-C-S-C	FEM	31.75	63.11	70.88	100.1	116.0

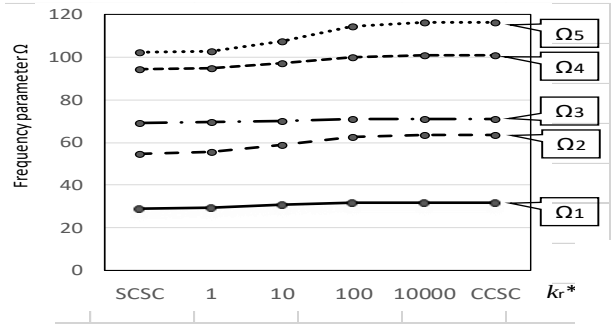

Figure 7 Variation of frequency parameters of square plate with spring stiffness (**Ex.5**).

Table 8 Frequency parameters Ω of square plates

(**Ex.6**, RS-C-C-C, ν =0.3)

kr^*		Ω_1	Ω_2	Ω_3	Ω_4	Ω_5
(0)	Ritz	31.83	63.33	71.08	100.8	116.4
S-C-C-C	FEM	31.75	63.11	70.88	100.1	116.0
1	Ritz	32.25	64.06	71.25	101.2	117.2
	FEM	32.17	63.85	71.05	100.5	116.8
10	Ritz	34.04	67.84	72.11	103.8	122.2
	FEM	33.97	67.63	71.90	103.0	121.8
100	Ritz	35.65	72.33	73.14	107.3	129.7
	FEM	35.57	72.10	72.91	106.5	129.3
10000	Ritz	35.98	73.38	73.39	108.2	131.6
	FEM	35.90	73.15	73.16	107.4	131.1
(infinity)	Ritz	35.99	73.39	73.39	108.2	131.6
C-C-C-C	FEM	35.89	73.15	73.15	107.4	131.1

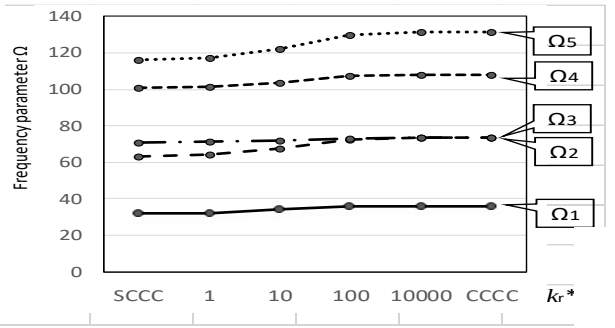

Figure 8 Variation of frequency parameters of square plate with spring stiffness (**Ex.6**).

Table 9 Frequency parameters Ω of square plates

(**Ex.7**, RS-RS-S-S, ν=0.3)

kr^*		Ω_1	Ω_2	Ω_3	Ω_4	Ω_5
S-S-S-S	Ritz	19.74	49.35	49.35	78.96	98.70
1	Ritz	20.62	50.27	50.27	79.89	99.64
10	Ritz	23.96	54.67	54.79	84.83	105.0
100	Ritz	26.55	59.44	59.68	91.19	112.5
10000	Ritz	27.05	60.53	60.78	92.82	114.5
C-C-S-S	Ritz	27.05	60.54	60.79	92.84	114.6

Table 10 Frequency parameters Ω of square plates

(**Ex.8**, RS-RS-C-S, ν=0.3)

kr^*		Ω_1	Ω_2	Ω_3	Ω_4	Ω_5
S-S-C-S	Ritz	23.65	51.67	58.65	86.13	100.3
1	Ritz	24.58	52.62	59.59	87.09	101.2
10	Ritz	28.25	57.19	64.33	92.23	106.6
100	Ritz	31.24	62.18	69.79	99.0	114.3
10000	Ritz	31.82	63.32	71.06	100.8	116.3
C-C-C-S	Ritz	31.83	63.33	71.08	100.8	116.4

Table 11 Frequency parameters Ω of square plates

(**Ex.9**, RS-RS-C-C, ν=0.3)

kr^*		Ω_1	Ω_2	Ω_3	Ω_4	Ω_5
S-S-C-C	Ritz	27.05	60.54	60.79	92.84	114.6
1	Ritz	28.04	61.54	61.72	93.82	115.5
10	Ritz	32.00	66.46	66.48	99.14	121.0
100	Ritz	35.32	72.07	72.07	106.3	129.3
10000	Ritz	35.98	73.38	73.38	108.2	131.6
C-C-C-C	Ritz	35.99	73.39	73.39	108.2	131.6

Table 12 Frequency parameters Ω of square plates

(**Ex.10**, RS-S-RS-S, ν=0.3)

kr^*		Ω_1	Ω_2	Ω_3	Ω_4	Ω_5
S-S-S-S	Ritz	19.74	49.35	49.35	78.96	98.70
1	Ritz	20.64	49.72	50.83	79.90	98.89
10	Ritz	24.51	51.65	58.25	85.09	100.0
100	Ritz	28.17	54.11	67.13	92.52	101.7
10000	Ritz	28.94	54.74	69.30	94.56	102.2
C-S-C-S	Ritz	28.95	54.74	69.33	94.59	102.2

Table 13 Frequency parameters Ω of square plates

(**Ex.11**, RS-C-RS-S, ν=0.3)

kr^*		Ω_1	Ω_2	Ω_3	Ω_4	Ω_5
S-C-S-S	Ritz	23.65	51.67	58.65	86.13	100.3
1	Ritz	24.40	53.09	58.96	87.00	101.9
10	Ritz	27.78	60.25	60.61	91.81	111.6
100	Ritz	31.10	62.76	68.92	98.81	115.9
10000	Ritz	31.82	63.32	71.05	100.8	116.4
C-C-C-S	Ritz	31.83	63.33	71.08	100.8	116.4

of simple support (without spring) and clamped edges. Ex.13 and 14 have three edges with rotational springs, and Ex.15 is a simply supported plate with all edges constrained by rotational springs.

Convergence study is presented in Table 1 for frequency parameters in Ex.1 obtained by the present (a) Ritz method and (b) finite element method. In both sets of results, non-dimensional spring constants are assumed as kr*=100 and 10000. In (a), the number of series terms in Eq.(14) are taken as $M\times N$= 6×6, 8×8 and 10×10, and very fast convergence from above (i.e., this solution is upper-bounded) is observed within the four significant figures. In (b), the number of finite elements is taken as 10×10, 15×15 and 20×20, and slightly slower convergence from below is observed as compared to the Ritz solution. This non-conforming finite element solution seems to give lower bound in this problem, but no theoretical proof is possible due to use of this non-conforming element. The discrepancy between the Ritz 10×10 solution and FEM 20×20 solution is 0.60 percent in the maximum and 0.29 percent on the average. Generally both different solutions agree well.

Table 2 presents a comparison in Ex.15 (uniformly constrained on the four edges) between Refs.[16,17] by Li and co-workers and the present Ritz result. The present solution here is given in the five significant figure to match to the result [17], and clearly they show excellent agreement. Thus in both Tables 1 and 2, validity of the present two methods is well established.

3.2. Frequency parameters of square plates

Tables 3-8 present pairs of frequency parameters obtained by the two different methods for the lowest five modes of square plates (a/b=1) in Ex.1-Ex.6, respectively. The degree of rotational springs is increased as k_r^*=0 (totally simply supported edge), 1, 10, 100, 10000 (almost clamped). In the limiting case of $k_r^*=\infty$ (infinity), the accurate values are available by replacing $k_r^*=\infty$ (S) with clamped edge (C). It is seen in common that the frequencies are monotonically increasing, as RS edge starts from simple support (k_r^*=0) to strongly constrained edge k_r^*=10000=10^4, and this degree of $k_r^*=10^4$ virtually coincide with the clamped edge.

Such monotonical increases in frequency can be seen in the accompanying Figs.3-8 for Ex-1-Ex.6, respectively. Some interesting observations are made in each figure. For example, in Fig.3 (Table 3), the second and third frequencies of S-S-S-S plate are identical (degenerated mode of a square plate) for k_r^*=0, but they become separated as k_r^* being increased and become the second and third frequencies of C-S-S-S plate. In contrast in Fig.8 (Table 8), two distinct second and third frequencies of S-C-C-C plate gradually approach each other and eventually merge into one degenerated mode.

Tables 9-17 list the lowest five frequencies obtained by the Ritz method only, when needed, they can be plotted in figures by using Excel and other software. When one needs frequency value for intermediate stiffness, one can introduce interpolation curves with respect to the stiffness values of k_r^*=0, 1, 10, 100, 10000 and ∞.

Table 14 Frequency parameters Ω of square plates

(**Ex.12**, RS-C-RS-C, ν=0.3)

k_r^*		Ω_1	Ω_2	Ω_3	Ω_4	Ω_5
S-C-S-C	Ritz	28.95	54.74	69.33	94.59	102.2
1	Ritz	29.57	56.08	69.59	95.37	103.9
10	Ritz	32.42	62.91	71.01	99.80	113.3
100	Ritz	35.33	71.29	72.89	106.3	127.7
10000	Ritz	35.98	73.37	73.39	108.2	131.6
C-C-C-C	Ritz	35.99	73.39	73.39	108.2	131.6

Table 15 Frequency parameters Ω of square plates

(**Ex.13**, RS-RS-RS-S, ν=0.3)

k_r^*		Ω_1	Ω_2	Ω_3	Ω_4	Ω_5
S-S-S-S	Ritz	19.74	49.35	49.35	78.96	98.70
1	Ritz	21.07	50.46	51.01	80.36	99.74
10	Ritz	26.33	55.86	59.17	87.87	105.6
100	Ritz	30.88	61.90	68.73	98.0	114.1
10000	Ritz	31.81	63.31	71.05	100.8	116.3
C-C-C-S	Ritz	31.83	63.33	71.08	100.8	116.4

Table 16 Frequency parameters Ω of square plates

(**Ex.14**, RS-RS-RS-C, ν=0.3)

k_r^*		Ω_1	Ω_2	Ω_3	Ω_4	Ω_5
S-S-S-C	Ritz	23.65	51.67	58.65	86.13	100.3
1	Ritz	24.95	53.32	59.75	87.52	102.1
10	Ritz	30.29	61.45	65.30	95.04	112.2
100	Ritz	35.00	71.03	71.82	105.4	127.5
10000	Ritz	35.98	73.37	73.37	108.2	131.5
C-C-C-C	Ritz	35.99	73.39	73.39	108.2	131.6

Table 17 Frequency parameters Ω of square plates

(**Ex.15**, RS-RS-RS-RS, ν=0.3)

k_r^*		Ω_1	Ω_2	Ω_3	Ω_4	Ω_5
S-S-S-S	Ritz	19.74	49.35	49.35	78.96	98.70
1	Ritz	21.50	51.19	51.19	80.83	100.6
10	Ritz	28.50	60.22	60.22	90.81	111.2
100	Ritz	34.67	70.78	70.78	104.5	127.0
10000	Ritz	35.97	73.36	73.36	108.2	131.5
C-C-C-C	Ritz	35.99	73.39	73.39	108.2	131.6

3.3. Frequency parameters of rectangular plates

Plate planform other than a square is considered to see the effect of aspect ratios. Tables 18 and 19 are sets of the lowest five frequencies for aspect ratios of a/b=2/3 and 1.5, respectively. Examples are taken form Ex.1 (one edge constrained by rotational spring), Exs.7 and 10 (two edges

Table 18 Frequency parameters Ω of rectangular plate (a/b=2/3, v=0.3)

kr*		Ω_1	Ω_2	Ω_3	Ω_4	Ω_5
Ex.1 RS-S-S-S						
0	Ritz	14.26	27.42	43.87	49.35	57.02
1	Ritz	14.86	27.74	44.70	49.53	57.67
10	Ritz	17.05	29.14	48.69	50.43	60.93
100	Ritz	18.62	30.41	51.44	52.86	64.72
10000	Ritz	18.90	30.66	51.67	53.77	65.61
C-S-S-S	Ritz	18.90	30.67	51.67	53.78	65.62
Ex.7 RS-RS-S-S						
S-S-S-S	Ritz	14.26	27.42	43.87	49.35	57.02
1	Ritz	15.03	28.12	44.76	50.03	57.86
10	Ritz	17.73	31.03	49.00	53.28	61.98
100	Ritz	19.61	33.52	53.40	56.74	66.68
10000	Ritz	19.95	34.02	54.35	57.50	67.78
C-C-S-S	Ritz	19.95	34.02	54.36	57.51	67.79
Ex.10 RS-S-RS-S						
S-S-S-S	Ritz	14.26	27.42	43.87	49.35	57.02
1	Ritz	15.47	28.07	45.52	49.72	58.31
10	Ritz	20.22	31.14	51.65	53.58	64.99
100	Ritz	24.23	34.37	54.11	62.80	73.44
10000	Ritz	25.04	35.10	54.74	64.98	75.58
C-S-C-S	Ritz	25.04	35.10	54.74	65.01	75.61
Ex.13 RS-RS-RS-S						
S-S-S-S	Ritz	14.26	27.42	43.87	49.35	57.02
1	Ritz	15.64	28.45	45.58	50.21	58.50
10	Ritz	20.81	32.92	53.86	54.44	65.98
100	Ritz	25.01	37.17	59.18	63.26	75.20
10000	Ritz	25.85	38.08	60.29	65.48	77.51
C-C-C-S	Ritz	25.86	38.09	60.30	65.51	77.53
Ex.15 RS-RS-RS-RS						
S-S-S-S	Ritz	14.26	27.42	43.87	49.35	57.02
1	Ritz	15.81	28.83	45.64	50.70	58.69
10	Ritz	21.52	34.83	54.18	57.30	67.04
100	Ritz	26.08	40.48	63.81	64.75	77.22
10000	Ritz	26.99	41.69	66.10	66.50	79.78
C-C-C-C	Ritz	27.01	41.70	66.12	66.52	78.81

Table 19 Frequency parameters Ω of rectangular plate (a/b=1.5, v=0.3)

kr*		Ω_1	Ω_2	Ω_3	Ω_4	Ω_5
Ex.1 RS-S-S-S						
S-S-S-S	Ritz	32.08	61.69	98.70	111.0	128.3
1	Ritz	32.36	62.28	98.79	111.8	128.6
10	Ritz	33.60	65.35	99.31	116.2	130.3
100	Ritz	34.79	69.03	100.1	122.8	133.0
10000	Ritz	35.05	69.90	100.3	124.6	133.8
C-S-S-S	Ritz	35.05	69.91	100.3	124.6	133.8
Ex.7 RS-RS-S-S						
S-S-S-S	Ritz	32.08	61.69	98.70	111.0	128.3
1	Ritz	33.29	62.78	100.1	112.1	129.6
10	Ritz	38.63	68.31	107.8	118.0	137.1
100	Ritz	43.77	74.91	119.2	126.9	149.0
10000	Ritz	44.88	76.53	122.3	129.4	152.5
C-C-S-S	Ritz	44.89	76.55	122.3	129.4	152.5
Ex.10 RS-S-RS-S						
S-S-S-S	Ritz	32.08	61.69	98.70	111.0	128.3
1	Ritz	32.64	62.88	98.89	112.6	128.9
10	Ritz	35.36	69.17	99.98	121.4	132.4
100	Ritz	38.38	77.38	101.7	135.5	138.3
10000	Ritz	39.08	79.50	102.2	139.6	140.2
C-S-C-S	Ritz	39.09	79.53	102.2	139.6	140.2
Ex.13 RS-RS-RS-S						
S-S-S-S	Ritz	32.08	61.69	98.70	111.0	128.3
1	Ritz	33.57	63.38	100.2	112.8	129.9
10	Ritz	40.17	71.98	108.5	123.2	139.1
100	Ritz	46.70	82.72	120.6	139.2	153.8
10000	Ritz	48.14	85.46	123.9	143.9	158.2
C-C-C-S	Ritz	48.16	85.49	124.0	144.0	158.3
Ex.15 RS-RS-RS-RS						
S-S-S-S	Ritz	32.08	61.69	98.70	111.0	128.3
1	Ritz	34.51	63.88	101.4	113.1	130.9
10	Ritz	45.58	75.17	117.0	125.1	145.9
100	Ritz	57.77	89.86	141.4	144.0	171.3
10000	Ritz	60.73	93.79	148.7	149.6	179.5
C-C-C-C	Ritz	60.76	93.83	148.8	149.7	179.6

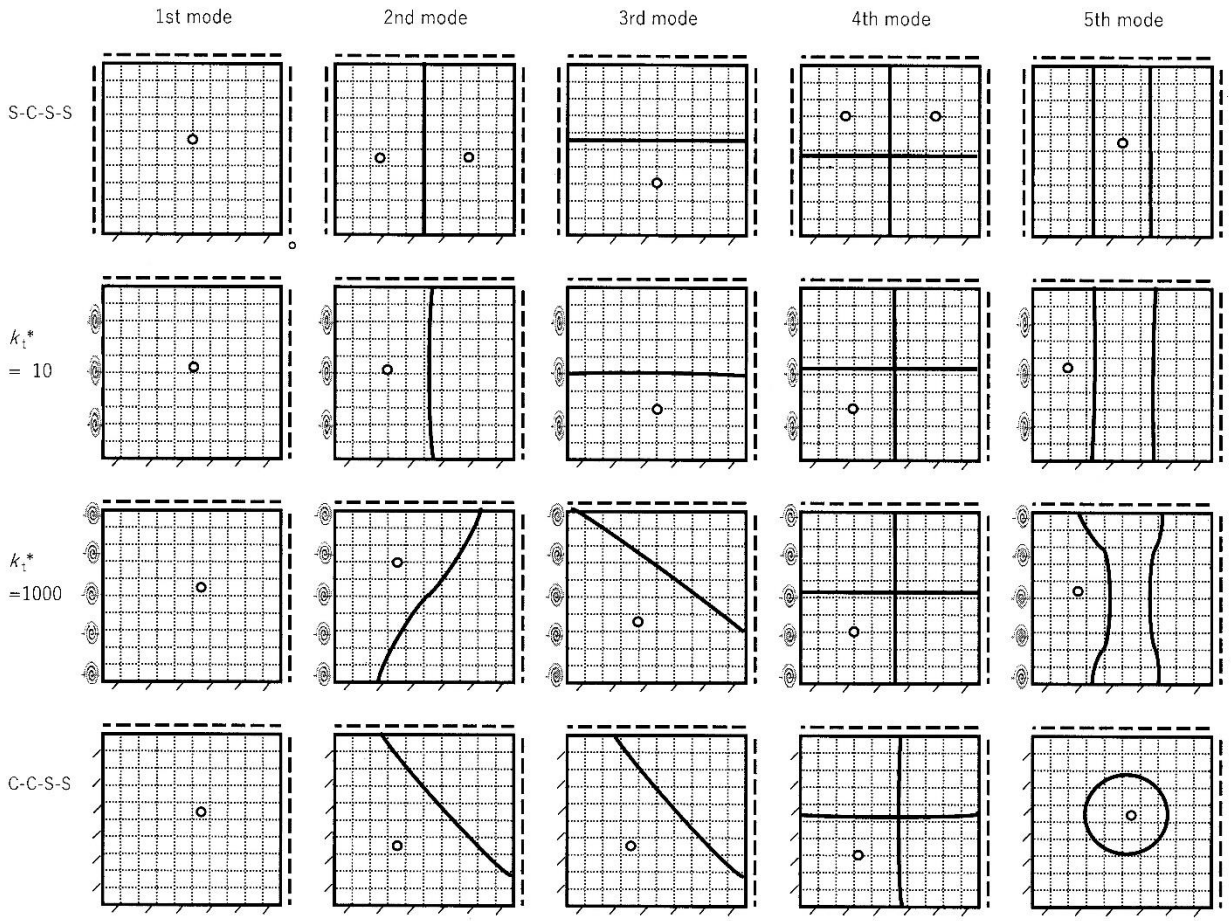

Figure 9 Mode shapes (nodal lines) of square plates (**Ex.2**) (○: Maximum amplitude)

by rotational springs), Ex.13 (three edges) and Ex.15 (four edges), where all examples here start from S-S-S-S plate. Since the present frequency parameter uses the side length a along x axis (Fig.1) in Eq.(12), a rectangular plate (a/b=2/3) appears to have more area than a plate (a/b=1.5), and therefore frequency values of a/b=2/3 in Table 18 have lower values than those of the smaller plate of a/b=1.5. The frequency values for other aspect ratios may be approximated by three-point interpolation or extrapolation curves using values for a/b=2/3, 1 and 1.5 in the paper.

3.4. Vibration mode of square plates

In free vibration analysis, vibration mode shapes are also important technical information. Nodal lines (line of zero amplitude) are plotted in Fig.9, as one example, for a square plate with one rotational spring on Edge(1) (Ex.2 in Fig.2). Variations of nodal lines are illustrated starting from kr*=0 (S-C-S-S plate) to kr*=∞ (C-C-S-S plate) by increasing rotational spring stiffness as kr*=10 and 1000. The maximum amplitude and nodal line are given as a circle ○ and thick solid lines in each figure.

All the first modes are (m*,n*)=(1,1) mode, where m* and n* are half wave numbers to describe modal shapes. There appear no nodal lines in the fundamental modes. The second and third modes are (2,1) and (1,2) modes, respectively. As the stiffness kr* is increased, nodal lines start skewed, and eventually these two modes merge and degeneration of (2,1) and (1,2) mode occurs to show the same nodal pattern. The fourth mode is (2,2) mode and nodal lines are kept almost straight and do not deform much. The fifth mode is (3,1) mode and nodal lines are skewed due to the stiffness increase. A nodal circle is formed by superposing (3,1) and (1,3) mode, as observed for totally clamped (C-C-C-C) square plate [1].

4. Conclusions

The present paper has illustrated a straightforward application of Ritz method to accurately determine the natural frequencies of a rectangular plate with uniform rotational elastic springs located on any of the four edges. A set of additional energy terms due to the springs was added to the plate strain energy in bending. The effects of the rotational springs on determining frequencies of the simply supported rectangular plates were comprehensively investigated through numerical results, including careful convergence and comparison studies. Accurate frequencies were tabulated for all the possible combinations of rotationally constrained edge(s) and other simply supported or clamped edges. It is expected that the comprehensive data is useful for researchers and design engineers.

References

1. Leissa AW, Vibration of Plates, NASA-SP-160, (1969). https://ntrs.nasa.gov/citations/19700009156
2. Gorman DJ, Vibration analysis of plates by the superposition method, World Scientific Pub, (1999).
3. Leissa AW, The free vibration of rectangular plates, *J. Sound Vib*., 31(1973), pp.257-293.
4. Narita Y, Natural frequencies of rectangular plates in improved accuracy, *EPI IJE*, 5 (2022), pp.26-36.
5. Laura PAA, Romanelli E, Vibrations of rectangular plates elastically restrained against rotation along all edges and subject to a bi-axial state of stress, *J. Sound Vibr*., 37 (1974), pp.367-377.
6. Gianetti CE, Diez L, Laura PAA, Transverse vibrations of rectangular plates with elastically restrained edges and subject to in-plane, shear forces, *J. Sound Vibr*., 54 (1977), pp.409-417.
7. Laura PAA, Grossi R, Transverse vibration of a rectangular plate elastically restrained against rotation along three edges and free on the fourth edge, *J. Sound Vibr*., 59 (1978), pp.355-368.
8. Laura PAA, Grossi R, Transverse vibrations of rectangular anisotropic plates with edges elastically restrained against rotation, *J. Sound Vibr*., 64 (1979), pp.257-267.
9. Bapat AV, Venkatramani, Simulation of classical edge conditions by finite elastic restraints in the vibration analysis of plates, *J. Sound Vibr*., 120 (1988), pp.127-140.
10. Grossi RO, Bhat RB, Natural frequencies of edge restrained tapered rectangular plates, *J. Sound Vibr.*, 185 (1995), pp.335-343.
11. Gorman DJ, A comprehensive study of the free vibration of rectangular plates resting on symmetrically-distributed uniform elastic edge supports, *J. Appl. Mech*. ASME, 56 (1989), pp.893-899.
12. Gorman DJ, A general solution for the free vibration of rectangular plates resting on uniform elastic edge supports, *J. Sound Vibr*., 139 (1990), pp.325-335.
13. Gorman DJ, The superposition method for free vibration analysis of rectangular plates with elastic edge support , Finite Elements in Analysis and Design, 18 (1994), pp.155-168.
14. Gorman DJ, A general solution for the free vibration of rectangular plates with arbitrarily distributed lateral and rotational elastic edge support, *J. Sound Vibr*., 174 (1994), pp.451-459.
15. Gorman DJ, Free vibration and buckling of in-plane loaded plates with rotational elastic edge support, *J. Sound Vibr*., 229 (2000), pp.755-773.
16. Li KM, Yu Z, A simple formula for predicting resonant frequencies of a rectangular plate with uniformly restrained edges, *J. Sound Vibr*., 327 (2009), pp.254-268.
17. Li WL, Zhang X., Du J, Liu Z, An exact series solution for the transverse vibration of rectangular plates with general elastic boundary supports, *J. Sound Vibr.*, 321 (2009), pp.254-269.
18. Eftekhari SA, Jafari AA, Accurate variational approach for the free vibration of variable thickness thin and thick plates with edges elastically restrained against translation and rotation, *Int. J. Mech. Sci.*, 68 (2013), pp.35-46.
19. Wan Z, Free vibration analysis of rectangular plates with arbitrary elastic boundary conditions, *INCE Conference Proceedings*, *InterNoise21*, (2021), pp.1891-1898, doi: //doi.org/10.3397/IN-2021-1985.
20. Zhang J, Lu J, Ullah S, Gao Y, Zhao D, Jamal A, Civalek O, Free vibration analysis of thin rectangular plates with two adjacent edges rotationally-restrained and the others free using finite Fourier integral transform method, *Struct. Engng. Mech.*, 80 (2021), pp.455-462.
21. Leng B, Ullah S, Yu T, Li K, New analytical free vibration solutions of thin plates using the Fourier series method, *Appl. Sci*., 12 (2022) , doi.org/10.3390/app12178631.
22. Narita Y, Vibration analysis of free rectangular plates constrained by translational edge spring, *EPI IJE*, 6 (2023), pp.9-17.
23. Narita Y, Combinations for the free-vibration behaviors of anisotropic rectangular plates under general edge conditions, *J. Appl. Mech. ASME*, 67 (2000), pp.568-573.
24. Narita Y, Polya counting theory applied to combination of edge conditions for generally shaped isotropic plates, *EPI IJE*, 2 (2019), pp.194-202.
25. Narita Y, Maximum frequency design of laminated plates with mixed boundary conditions, *Int. J. Solids Struct*., 43 (2006), pp. 4342–4356.